

Superfluid properties of a honeycomb dipolar supersolid

Albert Gallemí¹ and Luis Santos¹

¹*Institut für Theoretische Physik, Leibniz Universität Hannover, 30167 Hannover, Germany*

(Dated: September 22, 2022)

Recent breakthrough experiments on dipolar condensates have reported the creation of supersolids, including two-dimensional arrays of quantum droplets. Droplet arrays are, however, not the only possible non-trivial density arrangement resulting from the interplay of mean-field instability and quantum stabilization. Several other possible density patterns may occur in trapped condensates at higher densities, including the so-called honeycomb supersolid, a phase that exists, as it is also the case of a triangular droplet supersolid, in the thermodynamic limit. We show that compared to droplet supersolids, honeycomb supersolids have a much-enhanced superfluid fraction while keeping a large density contrast, and constitute in this sense a much better dipolar supersolid. However, in contrast to droplet supersolids, quantized vortices cannot be created in a honeycomb supersolid without driving a transition into a so-called labyrinthic phase. We show that the reduced moment of inertia, and with it the superfluid fraction, can be however reliably probed by studying the dynamics following a scissors-like perturbation.

I. INTRODUCTION

The recent realization of the supersolid phase in ultracold dipolar quantum gases [1–3] opens intriguing questions about the superfluidity in these systems [4]. The interplay between mean-field interactions, quantum fluctuations, and external confinement results in a rich landscape of possible density patterns, depending on the atom-atom interactions, the density, and the external trap [5–8]. Of these possible patterns, droplet arrays have been the most intensively explored phase. Dipolar droplet supersolids (D-SS) have been realized in recent years both in one- [1–3] and two-dimensional [9, 10] arrangements. In two dimensions, quantum droplets arrange in a triangular crystalline-like order, surrounded by a low-density region that ensures phase coherence amongst the different droplets.

Whereas most of the predicted density patterns demand an external confinement, in addition to the D-SS, only another modulated phase may occur in homogeneous space [6], namely the so-called honeycomb supersolid (H-SS). This pattern consists of a condensate containing hexagonally-arranged density holes, constituting the complementary pattern to the triangular droplet array. The observation of the H-SS demands significantly larger densities than the D-SS. Although this is still an important limitation in current experiments based on magnetic atoms, the problem could be circumvented with a tight confinement [7, 8], and could be much less relevant in future experiments with condensates of polar molecules [11].

Although recent experiments have revealed the expected presence of two different Goldstone modes associated with the phase coherence and the crystalline order [12–14], a direct clear proof of superfluid effects in dipolar supersolids is still lacking. Whereas in standard condensates the study of the scissors mode frequency provides a clear information about the reduction of the moment of inertia, and with it about superfluidity [15, 16], recent studies have revealed that a more subtle analysis

of the scissors response is necessary in D-SSs [17–19]. An alternative would be provided by the observation of quantized vortices. Recent studies have shown that vortices may be robustly created in D-SSs, where they occupy the inter-droplet interstitials [20–22]. Vortices have not yet been observed in a D-SS, but the recent experimental creation of vortices in an unmodulated dipolar condensate [23] opens optimistic perspectives in this direction.

These recent works on dipolar density patterns and on superfluid effects in D-SSs lead to intriguing questions about the superfluidity of other density patterns, and very especially of the H-SS, and about how the superfluidity of this phase may be experimentally revealed. This paper is devoted to these questions. We show that the H-SS has for a large contrast of the density modulation a much larger superfluid fraction than the D-SS. However, contrary to the D-SS, the H-SS is not robust when vortices nucleate, rather transitioning into a labyrinthic phase. Fortunately, the large superfluid fraction of the H-SS could be revealed under realistic conditions by a careful analysis of the scissors response.

The paper is organized as follows. In Sec. II, we introduce the formalism employed, and review the possible ground-state density patterns. Section III is devoted to the study of the density patterns under rotation. In Sec. IV, we analyze the moment of inertia of the different patterns, paying special attention to the H-SS. Section V discusses in detail how the response to a scissors perturbation may be employed to provide a good estimation of the reduction of the moment of inertia in the H-SS, revealing its large superfluid fraction. Our conclusions are summarized in Sec. VI.

II. GROUND-STATE PATTERNS

In the following, we consider a condensate of N bosons with mass m and magnetic dipole moment μ oriented along the z direction. A similar physics is expected for the case of electric dipoles, as it is in particular the case of

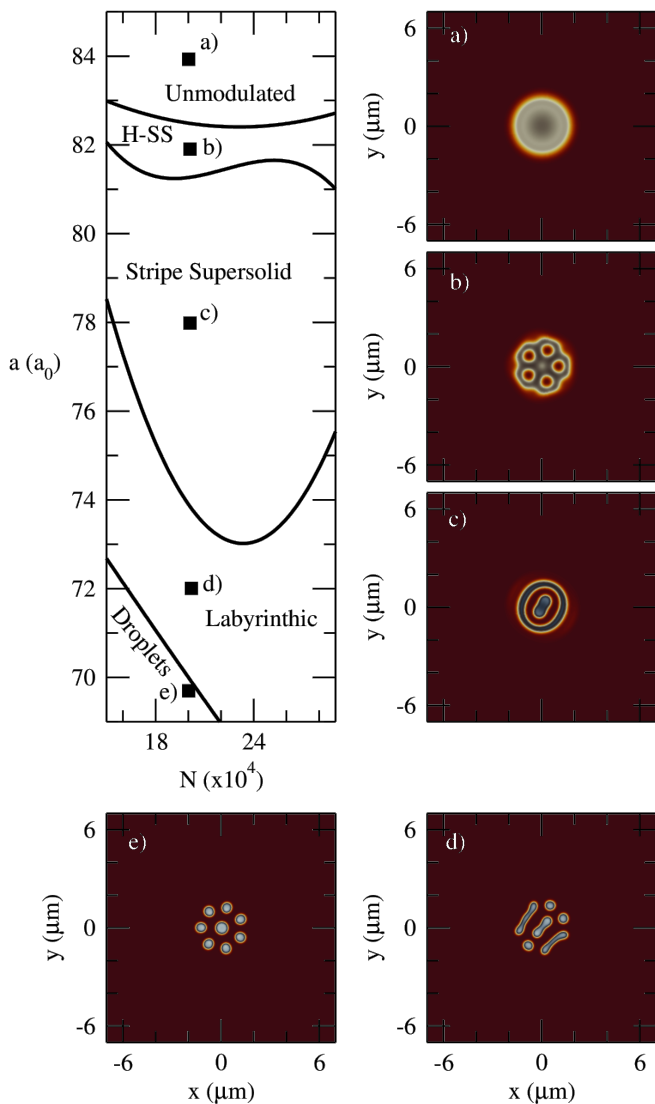


FIG. 1. (Top left) Ground-state phase diagram as a function of the scattering length and the atom number, for ^{162}Dy atoms confined in a harmonic trap with frequencies $\omega_{x,y,z} = 2\pi \times (200, 200, 400)$. The panels (a)-(e) show the density pattern in the xy plane for $N = 2 \times 10^5$ and $a/a_0 = 70, 72, 78, 82$ and 84 , which correspond to the droplet, labyrinthic, stripe, H-SS, and unmodulated patterns, respectively.

polar molecules [11]. The physics of a dipolar condensate is given by the interplay between contact interactions, characterized by the s -wave scattering length a , dipolar interactions, and (despite of its weakly-interacting character) quantum fluctuations. The latter provides the stabilization mechanism against mean-field collapse [24]. The physics of a quantum-stabilized dipolar condensate is well described by the so-called extended Gross-Pitaevskii

equation [25],

$$i\hbar\dot{\Psi}(\mathbf{r}, t) = \left[-\frac{\hbar^2}{2m}\nabla^2 + V_{\text{trap}}(\mathbf{r}) + g|\Psi(\mathbf{r}, t)|^2 + \int V_{\text{dd}}(\mathbf{r} - \mathbf{r}')|\Psi(\mathbf{r}', t)|^2 d\mathbf{r}' + \gamma|\Psi(\mathbf{r}, t)|^3 \right] \Psi(\mathbf{r}, t). \quad (1)$$

where $\Psi(\mathbf{r}, t)$ is the condensate wave function. In Eq. (1) $V_{\text{trap}}(\mathbf{r})$ is the external trapping of the system, $g = 4\pi\hbar^2 a/m$ is the coupling constant, $V_{\text{dd}} = \frac{\mu_0\mu^2}{4\pi} \frac{1-3\cos^2\theta}{|\mathbf{r}-\mathbf{r}'|^3}$ is the dipole-dipole interaction potential, with μ_0 the vacuum magnetic permeability, and θ the angle between $\mathbf{r} - \mathbf{r}'$ and the polarization direction. The last term of the equation accounts for the effects of quantum fluctuations, the so-called Lee-Huang-Yang correction [26], with

$$\gamma = \frac{16}{3\sqrt{\pi}} g a^{3/2} \text{Re} \left[\int_0^\pi d\phi \sin\phi [1 + \varepsilon_{\text{dd}}(3\cos^2\phi - 1)]^{\frac{5}{2}} \right], \quad (2)$$

where $\varepsilon_{\text{dd}} = g_{\text{dd}}/g$ is the ratio between the dipolar strength $g_{\text{dd}} = \mu_0\mu^2/3$ and the contact strength g . The ground state is obtained by setting in Eq. (1) $\Psi(\mathbf{r}, t) = e^{-i\mu t/\hbar}\Psi(\mathbf{r})$, with μ the chemical potential. Normalizing $\int d^3r |\Psi(\mathbf{r})|^2 = N$, we obtain $\Psi(\mathbf{r})$ using standard imaginary-time evolution techniques.

The interplay between dipole-induced mean-field instability, quantum stabilization, and external confinement results in a variety of possible ground state phases. If the condensate is mean-field stable, the density profile remains unmodulated, presenting (for sufficiently large interactions) a standard Thomas-Fermi parabolic form. We denote this phase in the following as the unmodulated phase. For a sufficiently low a , and small-enough N , the condensate is mean-field unstable, breaking into quantum droplets, which may remain coherently linked (super-solid regime) or eventually disconnected (independent-droplet regime). These phases have been experimentally observed both in quasi-one- ([1–3]) and quasi-2D geometries ([9, 10]). In the latter case, in the thermodynamic limit, the droplet pattern is expected to acquire a triangular geometry [6, 7, 10]. Recent works [5, 7] have shown, however, that the ground state phase diagram may be significantly richer for larger atoms numbers (for fixed external confinement). Particularly interesting is the so-called honeycomb phase, which as for the case of the triangular droplet array, extends all the way to the thermodynamic limit [6, 7]. This phase is characterized by the formation of empty regions, which are arranged in an hexagonal pattern. In the presence of harmonic confinement, a rich variety of additional patterns may occur, including the so-called labyrinthic, stripe, and pumpkin phases [5].

Figure 1 (top left panel) illustrates these possible ground-state phases for the particular case of a condensate of ^{162}Dy atoms (which possess a dipole moment $\mu = 10\mu_B$, μ_B being the Bohr magneton). We consider

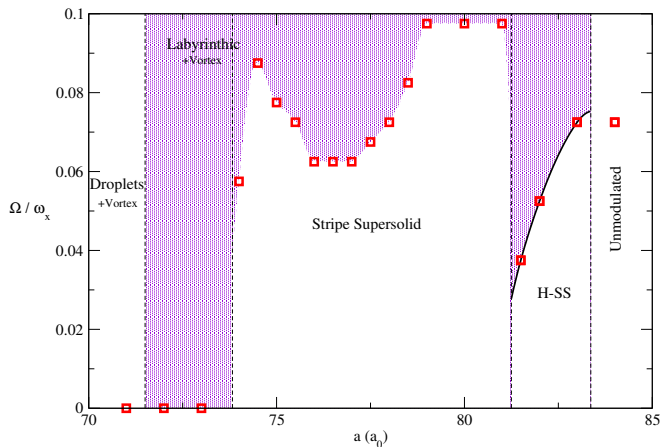


FIG. 2. Ground-state phase diagram of the system under rotation for $N = 2 \times 10^5$ as a function of the rotation frequency Ω , for the same parameters as in Fig. 1. Above a certain critical value of Ω (represented by the line in the plot and the red squares), a vortex nucleates. Note that for the stripe and the H-SS phases this results in the breaking of the pattern into a labyrinthine arrangement (shaded region).

throughout this paper an external harmonic confinement

$$V_{\text{trap}} = \frac{1}{2}m(\omega_x x^2 + \omega_y y^2 + \omega_z z^2), \quad (3)$$

with frequencies $\omega_{x,y} = \omega = 2\pi \times 200$ Hz and $\omega_z = 2\pi \times 400$ Hz. For N up to 3×10^5 atoms and $70 < a/a_0 < 84$, with a_0 the Bohr radius, the system presents different density patterns: unmodulated (panel (a)), H-SS (panel (b)), stripe phase (panel (c)) (formed by a pattern of concentric rings), labyrinthine (panel (d)) and droplet array (panel (e)). The so-called pumpkin pattern only appears in this case for much larger atom numbers [5].

III. ROBUSTNESS OF THE DENSITY PATTERN UNDER ROTATION

The creation of quantized vortices constitute a possible way to directly probe superfluidity. We consider at this point that the condensate is rotated around z with a rotation frequency Ω . We obtain the ground state by evaluating the eGPE in the rotating frame, minimizing $H - \Omega \hat{L}_z$, with \hat{L}_z the angular momentum operator along z . In the unmodulated phase, beyond a critical $\Omega > \Omega_c$, the solution with a vortex at the trap center becomes energetically favorable. In the presence of a density modulation, rotation does not only eventually result in the presence of vortices in the ground state, but may compromise as well the density pattern of the non-rotating ground state. In the D-SS phase, the ground state under rotation remains a droplet array (although the number of droplets may change), presenting, beyond a critical rotation frequency, vortices in the inter-droplet interstitials [20–22]. Interestingly, the situation is different for other density patterns.

We focus our attention on the particular case of $N = 2 \times 10^5$ atoms, which for the range of scattering lengths considered comprises all possible density patterns. Figure 2 depicts the ground state phase diagram as a function of Ω and a . As mentioned above, the droplet array is robust under rotation. In contrast, both the stripe phase and the H-SS are not. Increasing the rotation frequency results in a transition of the ground-state from a non-rotating stripe or H-SS pattern into a labyrinthine phase with a vortex. There is hence no ground state with a vortex with a stripe or H-SS pattern.

This has important consequences for the actual nucleation of vortices in experiments, which is typically realized by stirring the condensate by means of a slightly anisotropic rotating confinement on the xy plane. Although the solution without vortex is not the ground state, it remains metastable for $\Omega > \Omega_c$ because moving a vortex to the center of the trap demands overcoming a potential barrier [27]. Such a barrier is eventually circumvented for a sufficiently large rotational frequency, typically much larger Ω_c , at which the quadrupole surface mode is destabilized. This remains true also for a D-SS, although the critical rotation frequency for dynamical vortex nucleation may be significantly reduced compared to the unmodulated case [21].

In the D-SS phase, since the ground state under rotation remains a droplet array, the surface deformation is followed by the penetration of a vortex or vortices through the interstitials while keeping the droplet structure [20, 21]. The situation is radically different in the stripe and H-SS patterns, due to the absence of a ground state with a vortex in those cases. When the condensate is stirred at a rotation frequency high-enough to destabilize the quadrupole surface mode, the stripe and the honeycomb patterns are destroyed while vortices nucleate. Therefore, as expected from the ground-state properties discussed above, a labyrinthine pattern is formed with vortices in its interstitials. This is illustrated in Fig. 3. Starting with the non-rotating H-SS ground state for $a = 82a_0$ (left panel), we increase adiabatically Ω . The eventual surface deformation for rotational frequencies above the quadrupole frequency leads to the creation of a vortex or vortices, but, prior to that, also to the destruction of the honeycomb pattern (right panel).

As discussed below, the H-SS constitutes a much better supersolid than the droplet array. However, our results show that the lack of robustness of the density pattern under rotation is expected to prevent under typical experimental conditions the direct probe of superfluidity of that phase by means of the creation of quantized vortices. Fortunately, as shown in the following, the study of the moment of inertia constitutes a feasible alternative to directly probe the superfluidity of the H-SS.

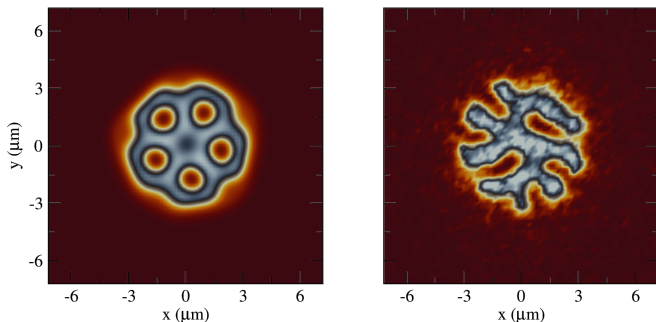


FIG. 3. (left panel) Initial condensate (without rotation) in the H-SS phase at $t = 0$ for $a = 82a_0$ (and the same parameters as Fig. 4). When the trap is rotated with a trap anisotropy $\delta = 0.025$ (see text) increasing adiabatically with a linear ramp of 0.03 ms the rotation frequency up to $\Omega = 0.9\omega_x$ (over the threshold frequency for the dynamical nucleation of vortices), the honeycomb pattern is destroyed into a labyrinthine arrangement, shown in the right panel at $t = 43$ ms.

IV. MOMENT OF INERTIA

The moment of inertia may be theoretically evaluated from the response to an infinitesimally slow rotation, as $I_{\text{exact}} = \lim_{\Omega \rightarrow 0} \frac{d\langle L_z \rangle}{d\Omega}$, where $\langle \hat{L}_z \rangle$ is the expected value of the angular momentum operator in the ground state calculated in the rotating frame. The reduction of the moment of inertia with respect to its classical value in a cylindrically-symmetric quantum gas, $I_C = m \int n(\mathbf{r})(x^2 + y^2) d\mathbf{r}$, is a clear signature of a finite superfluid fraction, which together with the density modulation, becomes a direct probe for supersolidity [4, 19, 20].

Figure 4(a) shows, for $N = 2 \times 10^5$, I_{exact}/I_C (black dots) as a function of a . The moment of inertia provides crucial information about the superfluid properties, although the lack of cylindrical symmetry may partially mask the true superfluid nature in some configurations. Due to the (quasi-)cylindrical symmetry of the unmodulated and stripe phases, the moment of inertia of these configurations turns out to be very close to zero. In both the labyrinth and the droplet patterns, the moment of inertia increases dramatically and approaches the classical rigid value, indicating the rigid response of the solid part. Most relevantly, the H-SS presents a very low moment of inertia, showing that, compared to the droplet array, it has typically a much larger superfluid fraction, while presenting a large density contrast.

V. SCISSORS-LIKE PERTURBATION

The reduction of the moment of inertia associated to superfluidity may be probed by monitoring the response of the system against a scissors-like perturbation. In the unmodulated phase, the frequency of the scissors mode

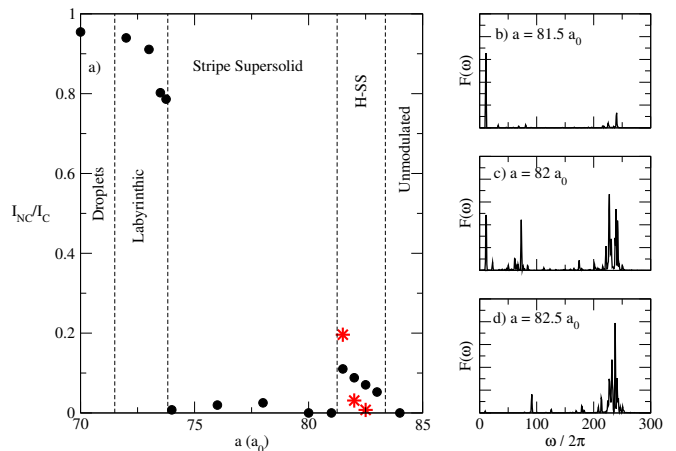


FIG. 4. (a) Moment of inertia I_{exact}/I_C (black dots) for $N = 2 \times 10^5$ atoms, as a function of the scattering lengths (all other parameters as in Fig. 4). Panels (b)-(d) show the Fourier transform $\mathcal{F}(\omega)$ of the signal $\langle xy \rangle(t)$ of the scissors mode (see text), measured after a sudden stop of a rotation of 1 Hz for $a/a_0 = 81.5, 82,$ and 82.5 , respectively. The estimation of the moment of inertia using Eq. (4) for those cases is indicated with red stars in panel (a).

may be directly linked to the superfluid fraction [15, 16]. As shown by recent experiments on dipolar condensates, the situation is more subtle in the case of a D-SS [17–19], since determining the dominant frequency of the scissors mode does not generally allow for a clear proof of global superfluidity. However, a careful study of the overall spectrum of the system response against the scissors-like perturbation may provide an experimental estimation of the reduction of the moment of inertia under proper conditions [19]. A similar procedure may be employed for the study of superfluidity in the H-SS.

We consider in the following a slightly deformed trap on the xy plane, with $\omega_{x,y} = \omega(1 \pm \delta)$, with $\delta = 0.025$. Two possible experimental procedures may be employed for the study of the moment of inertia. The scissors-like perturbation may be induced either by starting with the ground state and tilting the trap on the xy plane, or by rotating the condensate around z and then suddenly stopping the rotation. In both cases, we may monitor the scissors-mode response $\langle xy \rangle(t)$ as a function of time and obtain the Fourier transform within a given time window $0 < t < T$: $\mathcal{F}(\omega) = \int_0^T dt \langle xy \rangle(t) e^{i\omega t}$. Using sum rules, it is possible to show that the moment of inertia may be estimated as [19]:

$$I_p = m(\omega_y^2 - \omega_x^2) \langle x^2 - y^2 \rangle \frac{\int d\omega \mathcal{F}(\omega) \omega^{p-2}}{\int d\omega \mathcal{F}(\omega) \omega^p}, \quad (4)$$

with $p = 0$ ($p = 1$) for the tilting (rotation) protocol. Recent studies of the D-SS, have shown that both probing methods may in principle provide a reasonably good estimation of the moment of inertia. However, the tilting mechanism is particularly sensitive to low-frequency modes. As a result, that procedure demands

prohibitively long integration times in order to provide reliable estimations of the moment of inertia. In contrast, the study of the scissors mode after suddenly stopping the rotation is much less sensitive to low frequencies, and hence provides a much better alternative.

Similar procedures may be employed to study experimentally the moment of inertia in the H-SS. We have evaluated for $N = 2 \times 10^5$ atoms the system response during $T = 1$ s (the results are very consistent down to integration times as short as 200 ms, well within realistic experimental lifetimes). The tilting procedure is very much affected by the very low-frequency modes characteristic of the polar quasi-symmetry of the H-SS pattern. As a result, that procedure provides a very bad estimation of I_{exact}/I_C ; for $a = 82a_0$, the estimation is 5.36 versus the correct 0.08 value. A much better result is obtained using the rotation technique (see the red-star symbols, and panels (b) to (d) in Fig. 4). Note that, although there is still a deviation from the actual value, the absolute difference with the exact result is small. Hence, the rotation method can be experimentally applied to reveal the much larger superfluid fraction of the H-SS compared to that of the D-SS.

VI. CONCLUSIONS

Although research on dipolar supersolids has been limited up to now to the case of droplet supersolid arrays, experiments using larger number of atoms or tighter traps, or working with polar molecules, may open in the near future the possibility for studying other intriguing two-dimensional density patterns in quantum-stabilized dipolar condensates. Of those, honeycomb supersolids are particularly interesting, since, in contrast to droplet supersolids, their superfluid fraction remains very large even for a large density contrast. However, as discussed in this paper, the superfluidity of the honeycomb supersolid cannot be probed by the observation of quantized vortices due to the lack of robustness of the density pattern. Under rotation, vortex nucleation results in the destruction of the honeycomb pattern into a labyrinthic one. We have shown, however, that the large superfluid fraction of the honeycomb supersolid may be probed by a proper monitoring of the response after a scissors-like perturbation.

ACKNOWLEDGMENTS

We acknowledge support of the Deutsche Forschungsgemeinschaft (DFG, German Research Foundation) under Germany's Excellence Strategy—EXC-2123 QuantumFrontiers–390837967, and FOR 2247.

-
- [1] L. Tanzi, E. Lucioni, F. Famà, J. Catani, A. Fioretti, C. Gabbanini, R. N. Bisset, L. Santos, and G. Modugno, *Phys. Rev. Lett.* **122**, 130405 (2019).
 - [2] F. Böttcher, J.-N. Schmidt, M. Wenzel, J. Hertkorn, M. Guo, T. Langen, and T. Pfau, *Phys. Rev. X* **9**, 011051 (2019).
 - [3] L. Chomaz, D. Petter, P. Ilzhöfer, G. Natale, A. Trautmann, C. Politi, G. Durastante, R. M. W. van Bijnen, A. Patscheider, M. Sohmen, M. J. Mark, and F. Ferlaino, *Phys. Rev. X* **9**, 021012 (2019).
 - [4] A. J. Leggett, *Phys. Rev. Lett.* **25**, 1543 (1970).
 - [5] J. Hertkorn, J.-N. Schmidt, M. Guo, F. Böttcher, K. S. H. Ng, S. D. Graham, P. Uerlings, T. Langen, M. Zwierlein, and T. Pfau, *Phys. Rev. Research* **3**, 033125 (2021).
 - [6] Y.-C. Zhang, F. Maucher, and T. Pohl, *Phys. Rev. Lett.* **123**, 015301 (2019).
 - [7] Y.-C. Zhang, T. Pohl, and F. Maucher, *Phys. Rev. A* **104**, 013310 (2021).
 - [8] E. Poli, T. Bland, C. Politi, L. Klaus, M. A. Norcia, F. Ferlaino, R. N. Bisset, and L. Santos, *Phys. Rev. A* **104**, 063307 (2021).
 - [9] M. A. Norcia, C. Politi, L. Klaus, E. Poli, M. Sohmen, M. J. Mark, R. N. Bisset, L. Santos, and F. Ferlaino, *Nature* **596**, 357 (2021).
 - [10] T. Bland, E. Poli, C. Politi, L. Klaus, M. A. Norcia, F. Ferlaino, L. Santos, and R. N. Bisset, *Phys. Rev. Lett.* **128**, 195302 (2022).
 - [11] M. Schmidt, L. Lassablière, G. Quémener, and T. Langen, *Phys. Rev. Research* **4**, 013235 (2022).
 - [12] L. Tanzi, S. M. Roccuzzo, E. Lucioni, F. Famà, A. Fioretti, C. Gabbanini, G. Modugno, A. Recati, and S. Stringari, *Nature* **574**, 382 (2019).
 - [13] M. Guo, F. Böttcher, J. Hertkorn, J.-N. Schmidt, M. Wenzel, H. P. Büchler, T. Langen, and T. Pfau, *Nature* **574**, 386 (2019).
 - [14] G. Natale, R. M. W. van Bijnen, A. Patscheider, D. Petter, M. J. Mark, L. Chomaz, and F. Ferlaino, *Phys. Rev. Lett.* **123**, 050402 (2019).
 - [15] D. Guéry-Odelin and S. Stringari, *Phys. Rev. Lett.* **83**, 4452 (1999).
 - [16] O. M. Maragò, S. A. Hopkins, J. Arlt, E. Hodby, G. Hechenblaikner, and C. J. Foot, *Phys. Rev. Lett.* **84**, 2056 (2000).
 - [17] L. Tanzi, J. G. Maloberti, G. Biagioni, A. Fioretti, C. Gabbanini, and G. Modugno, *Science* **371**, 1162 (2021), <https://www.science.org/doi/pdf/10.1126/science.aba4309>.
 - [18] M. A. Norcia, E. Poli, C. Politi, L. Klaus, T. Bland, M. J. Mark, L. Santos, R. N. Bisset, and F. Ferlaino, *Phys. Rev. Lett.* **129**, 040403 (2022).
 - [19] S. M. Roccuzzo, A. Recati, and S. Stringari, *Phys. Rev. A* **105**, 023316 (2022).
 - [20] S. M. Roccuzzo, A. Gallemí, A. Recati, and S. Stringari, *Phys. Rev. Lett.* **124**, 045702 (2020).

- [21] A. Gallemí, S. M. Roccuzzo, S. Stringari, and A. Recati, *Phys. Rev. A* **102**, 023322 (2020).
- [22] M. Šindik, A. Recati, S. M. Roccuzzo, L. Santos, and S. Stringari, “Creation and robustness of quantized vortices in a dipolar supersolid when crossing the superfluid-to-supersolid transition,” (2022).
- [23] L. Klaus, T. Bland, E. Poli, C. Politi, G. Lamporesi, E. Casotti, R. N. Bisset, M. J. Mark, and F. Ferlaino, “Observation of vortices and vortex stripes in a dipolar bose-einstein condensate,” (2022).
- [24] D. S. Petrov, *Phys. Rev. Lett.* **115**, 155302 (2015).
- [25] F. Wächtler and L. Santos, *Phys. Rev. A* **93**, 061603 (2016).
- [26] A. R. P. Lima and A. Pelster, *Phys. Rev. A* **86**, 063609 (2012).
- [27] S. Sinha and Y. Castin, *Phys. Rev. Lett.* **87**, 190402 (2001).